Timing Ultrafast Charge Transfer via Fano Interference beyond the Core-Hole Clock

Ji-Cai Liu,[1,*] Nicolas Velasquez,[2,*,†] Victor Kimberg,[3] Sayantan Sarkar,[2] Oksana Travnikova,[2,4] Iyas Ismail,[2,4] Renaud Guillemin,[2,4] Man Zhang,[1] Pavel Krasnov,[5,6] Marcella Iannuzzi,[7] Michael Odelius,[8] Ralph Püttner,[9] Maria Novella Piancastelli,[2] Marc Simon,[2,4] Faris Gel'mukhanov,[3,‡] and Tatiana Marchenko[2,4,§]

[1]*School of Mathematics and Physics, North China Electric Power University, 102206 Beijing, China*
[2]*Sorbonne Université, CNRS, Laboratoire de Chimie Physique-Matière et Rayonnement, LCPMR, F-75005 Paris Cedex 05, France*
[3]*Department of Theoretical Chemistry and Biology, KTH Royal Institute of Technology, 10691 Stockholm, Sweden*
[4]*Synchrotron Soleil, L'Orme des Merisiers, Saint-Aubin, F-91192 Gif-sur-Yvette, France*
[5]*Federal Siberian Research Clinical Centre under the Federal Medical Biological Agency, 660037, Krasnoyarsk, Russia*
[6]*International Research Center of Spectroscopy and Quantum Chemistry–IRC SQC, Siberian Federal University, 660041, Krasnoyarsk, Russia*
[7]*Department of Chemistry, University of Zurich, Zurich 8057, Switzerland*
[8]*Department of Physics, Stockholm University, AlbaNova University Center, 10691 Stockholm, Sweden*
[9]*Fachbereich Physik, Freie Universität Berlin, Arnimallee 14, D-14195 Berlin, Germany*

(Received 18 November 2025; accepted 11 June 2026; published 28 July 2026)

Ultrafast charge transfer (CT) lies at the heart of molecular and electronic functionality. We develop a Fano-based core-hole clock (FCHC) method that captures coherent coupling between localized excitons and the directly populated delocalized CT continua in resonant Auger scattering. Applied to sulfur *KLL* Auger spectra of a conductive organic polymer, FCHC reveals clear Fano interference and a CT time of 27 ± 1.8 fs, demonstrating that the conventional core-hole clock model underestimates the CT dynamics timescale. We establish FCHC as a robust method for probing ultrafast CT in complex molecular systems.

DOI: 10.1103/h6h9-j83r

Charge transfer (CT), driven by coupled electronic and nuclear dynamics, is a fundamental process across physics, chemistry, and materials science due to its key role in energy and charge flow on the molecular scale [1,2]. A key challenge in complex systems is achieving spatial and temporal control over electron motion, which requires element-specific excitation. X-ray photons provide this capability by exciting a tightly bound core electron, creating a discrete, localized core exciton embedded in a manifold of delocalized electronic states. The x-ray absorption spectrum (XAS) of such a system contains two overlapping features: a narrow-band localized exciton and a broad-band delocalized CT continuum.

When a discrete state interacts with a continuum of states, their quantum amplitudes interfere, producing the characteristic asymmetric line shapes in the absorption spectra first described by Fano in 1961 [3]. This Fano interference is one of the most general manifestations of quantum coherence, governing phenomena as diverse as autoionization in atoms [3], transport through quantum dots [4], and light-matter coupling in plasmonic and photonic systems [5].

In core-level excitations of condensed systems, the discrete exciton and the delocalized CT continuum naturally form such a Fano-coupled system. The discrete core exciton state has two competing decay channels: intrinsic core-hole annihilation, which may occur via emission of a resonant Auger electron with rate Γ, and charge delocalization into the CT continuum with rate γ. Equally, the core-excited CT continuum can decay via Auger electron emission with rate Γ or via CT to the exciton with rate γ. The decay rates Γ and γ determine, respectively, the lifetime of the core-excited state $\tau_{\mathrm{CH}} = 1/2\Gamma$ and the CT time $\tau_{\mathrm{CT}} = 1/2\gamma$. The interplay between these channels defines the dynamics of CT, with the core-hole lifetime τ_{CH} serving as a natural internal clock [6–11]. This concept underlies core-hole clock (CHC) spectroscopy, where ultrafast processes are probed within the core-hole lifetime, ranging from a few femtoseconds to the attosecond regime [6,7,12–18].

Although conventional CHC spectroscopy is widely used to time ultrafast CT, its phenomenological framework is incomplete. The main limitation is the absence of a strict quantum-mechanical description of the resonant excitation and relaxation process that accounts for the interference between the discrete exciton and the continuum CT band in the core-excited state. The CHC model assumes that x-ray absorption populates only the excitonic state, with

*These authors contributed equally to this work.
†Present address: Molecular Physics, Fritz-Haber-Institut der Max-Planck-Gesellschaft, 14195 Berlin, Germany.
‡Contact author: faris@kth.se
§Contact author: tatiana.marchenko@sorbonne-universite.fr

subsequent depopulation via resonant Auger decay or CT [Fig. 1(a)]. This simplification neglects the coherent population of both localized exciton and delocalized CT states by an x-ray photon with different transition dipole moments d_{exc} and d_{CT}, which together form a Fano state [Fig. 1(b)]. Note that resonant Auger scattering (RAS), contrary to XAS offers a significant advantage allowing for the separation of excitonic and CT channels due to their qualitatively different dispersion laws [Fig. 1(c)] [6,7,12,19].

At first glance, the CT process may appear to involve charge exchange between the exciton and the CT continuum, rather than a purely unidirectional transfer. To clarify this issue, we examine the charge-flow dynamics in the core-excited state following excitation by a short x-ray pulse. Analysis of the electronic wave packet evolving in the core-excited state reveals exponential depopulation of the exciton with rate γ, arising from its coupling to the effectively infinite bath of the CT continuum. Accordingly, the CT time $\tau_{\mathrm{CT}} = 1/2\gamma$ characterizes a unidirectional charge transfer from the exciton to the CT continuum (see the Supplemental Material [20] for details). In the following, we demonstrate how this CT rate γ can be

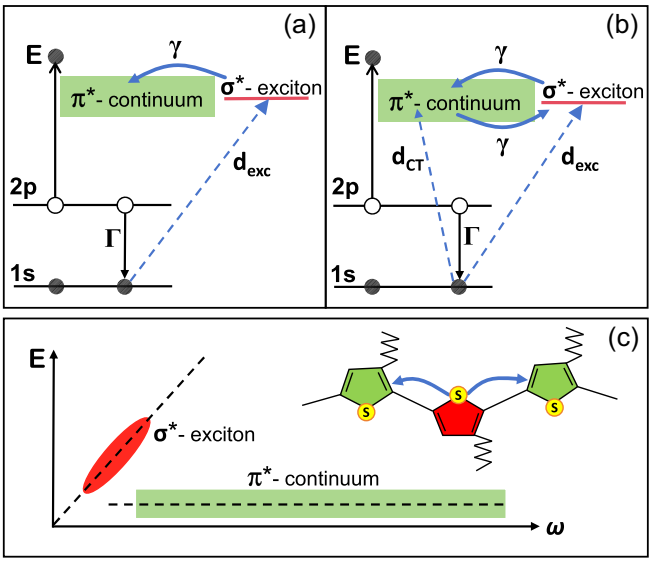

FIG. 1. Schematic of resonant Auger S $KL_{2,3}L_{2,3}$ transitions in the poly(3-hexylthiophene-2,5-diyl) (P3HT) polymer. (a) Conventional CHC model: x-ray absorption populates only the excitonic state σ^* exciton with transition dipole moment d_{exc}. Subsequent charge transfer to the π^* continuum with rate γ is accompanied by Auger decay of the core-excited state with the total rate Γ. (b) Fano-based CHC model: x-ray photon coherently populates localized σ^* exciton and delocalized π^* continuum with different transition dipole moments d_{exc} and d_{CT}, which together form a Fano state. Subsequent charge transfer between the interfering σ^* exciton and π^* continuum with rate γ is accompanied by Auger decay with total rate Γ. (c) Schematic dispersion laws of the exciton and CT channels in KLL Auger decay. The exciton channel displays Raman dispersion with photon energy, whereas the CT channel is nondispersive.

extracted from a RAS experiment performed with a continuous-wave x-ray field.

Here, we develop a strict quantum-mechanical Fano-based core-hole clock (FCHC) framework that explicitly includes this coherent exciton-continuum coupling in resonant Auger scattering. As an experimental test bed for our theory, we choose an organic conductive polymer poly(3-hexylthiophene-2,5-diyl) (P3HT), which due to its π-conjugated backbone enables efficient charge transfer and serves as a model system for probing charge transport in conjugated polymers [22]. Applied to the sulfur $KL_{2,3}L_{2,3}$ resonant Auger spectra of P3HT, FCHC reveals direct signatures of Fano interference and yields charge-transfer times far longer than predicted by the conventional CHC model. Our work demonstrates that Fano interference, being one of the most universal features of quantum systems, plays an equally fundamental role in ultrafast charge transfer in molecular materials.

To probe ultrafast CT dynamics in thin film P3HT, we measured resonant Auger S $KL_{2,3}L_{2,3}$ spectra at the SOLEIL French national synchrotron facility using the high-resolution HAXPES station for hard x-ray photoemission spectroscopy [23] located at the GALAXIES beamline [24]. The setup provided an electron energy resolution of 180 meV and photon bandwidth of 225 meV at 2.5 keV. The measurements were performed at close to normal incidence of the x-ray beam with polarization vector parallel to the sample surface. More experimental details can be found in Ref. [17].

The experimental 2D map (Fig. 2) shows the Auger electron spectra as a function of both the Auger electron kinetic energy E and the incident photon energy ω. The intensity is shown on a logarithmic color scale. The diagonal dashed lines show Raman dispersive Auger transitions from the $1s^{-1}\sigma^*$ and $1s^{-1}\pi^*$ excitons to the $2p^{-2}\sigma^*$ and $2p^{-2}\pi^*$ final states (labeled as σ^* exciton and π^* exciton). The maximum intensity of the σ^* exciton occurs at the resonant photon energy $\omega_{\mathrm{exc}} = 2473.3$ eV and corresponds to the resonant Auger electron energy $E_{\mathrm{exc}} = 2116$ eV. The horizontal dashed line shows a nondispersive Auger transition from the CT band to the $2p^{-2}$ final state at Auger electron energy $E_{\mathrm{CT}} = 2113$ eV (labeled as π^* continuum). Above the ionization threshold located around 2478 eV, the π^* continuum evolves into the normal Auger line. In contrast to the exciton RAS channel with Raman dispersion, the Auger electron energy in the CT channel is independent of the photon energy, except for a weak ω dependence below the ionization threshold caused by the spectator electron screening effect [17].

According to our earlier calculations [17], the spectrum of unoccupied levels in the P3HT polymer consists of quasicontinua formed by the σ^* and π^* subsystems. The interaction with the $1s$ core hole localized on the sulfur atom causes the σ^* exciton to split from the σ^* continuum and become embedded within the π^*

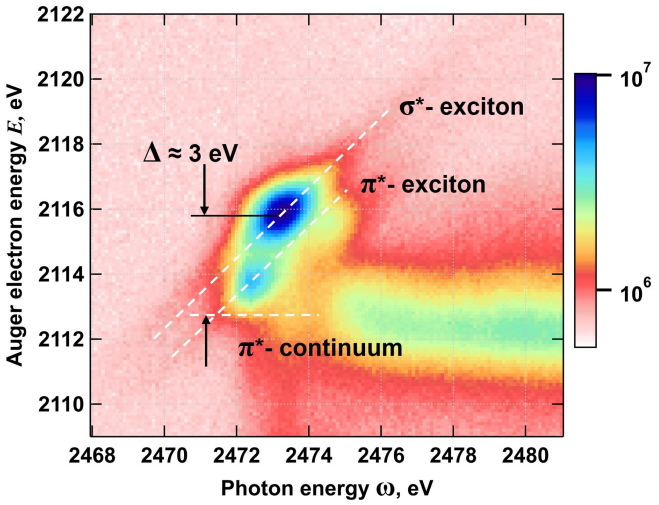

FIG. 2. 2D map of S $KL_{2,3}L_{2,3}$ RAS spectra recorded in thin film P3HT. Diagonal dashed lines show Raman dispersive Auger transitions from $1s^{-1}\sigma^*$ and $1s^{-1}\pi^*$ excitons to $2p^{-2}\sigma^*$ and $2p^{-2}\pi^*$ final states (σ^* exciton and π^* exciton), whereas the horizontal dashed line shows a nondispersive Auger transition from the CT band to the $2p^{-2}$ final state (π^* continuum), which evolves into a normal Auger line above the ionization threshold located around 2478 eV. Spectator shift $\Delta = 3$ eV quenching the Fano interference between the exciton and the CT channels in the final state is shown with arrows. The color-coded intensities are on logarithmic scale.

continuum. The nonplanar geometry of the P3HT polymer [25] allows coupling of the σ^* exciton to the π^* continuum, which enables the CT process (Fig. 1).

Conventionally, in the CHC method the CT time τ_{CT} is extracted by comparing the integrated intensities of the exciton $\sigma_{\mathrm{exc}}(\Omega) = p(\Omega)\Gamma/(\Gamma+\gamma)$ and CT $\sigma_{\mathrm{CT}}(\Omega) = p(\Omega)\gamma/(\Gamma+\gamma)$ RAS bands using the CHC equation [6,7]

$$\frac{\sigma_{\mathrm{exc}}(\Omega)}{\sigma_{\mathrm{CT}}(\Omega)} = \frac{\Gamma}{\gamma} = \frac{\tau_{\mathrm{CT}}}{\tau_{\mathrm{CH}}}, \tag{1}$$

where $\Omega = \omega - \omega_{\mathrm{exc}}$ is the detuning of the photon energy from the exciton resonance and $p(\Omega)$ is the absorption probability to the discrete exciton state. Here, we underline that the CT rate γ, and hence the CT time τ_{CT}, is an intrinsic property of the system, relevant for the particular exciton embedded in the continuum. Assuming a constant density of unoccupied states in the continuum, the CT time τ_{CT} is independent of the photon energy ω within the width of the exciton Γ. In the case where the density of states is not constant, the CT time τ_{CT} can show a smooth photon energy dependence. Consequently, within the framework of CHC theory, the ratio in Eq. (1) is expected to be Ω independent, and the cross section of the CT channel $\sigma_{\mathrm{CT}}(\Omega)$ should mirror the resonant Ω dependence of the exciton channel $\sigma_{\mathrm{exc}}(\Omega)$. However, a constant ratio in Eq. (1) is inappropriate to describe the experimentally observed strong dependence on the photon energy ω, which is often misinterpreted as a dependence of the CT time τ_{CT} on the excitation energy [12,16].

As mentioned above, the major shortcoming of CHC theory is that it neglects the direct population of the CT continuum and the coherent coupling between this continuum and the exciton in the core-excited state and thus overlooks a key part of the underlying physics. The parameter missing in Eq. (1) is the Fano shape parameter q, which is proportional to the transition dipole moments' ratio $d_{\mathrm{exc}}/d_{\mathrm{CT}}$, and quantifies the relative strength of the coherent pathways: large q corresponds to a dominant resonant transition to the discrete exciton and a weak direct transition to the continuum, while finite q points to a strong interference between the discrete and continuum states.

Below we derive expressions for the integral cross sections $\sigma_{\mathrm{exc}}(\Omega)$ and $\sigma_{\mathrm{CT}}(\Omega)$ based on Fano theory and compare them to the experimental data.

The RAS process consists of a core excitation $|0\rangle \to |c\rangle = |1s^{-1}\Psi^1_\epsilon\rangle$ to the coherent superposition of discrete exciton $|cn\rangle = |1s^{-1}\psi^1_{\mathrm{exc}}\rangle$ and CT continuum $|c\epsilon\rangle = |1s^{-1}\psi^1_{\mathrm{CT}}\rangle$ states. The coupling of these states results in Fano interference observed in XAS [26]. This is followed by Auger decay to the final spectator state $|c\rangle \to |f\rangle = |2p^{-2}\Psi^1_\epsilon\psi_E\rangle$, which in its turn is also a coherent superposition of exciton $|fn\rangle$ and CT $|f\epsilon\rangle$ states. Here ϵ is the energy of the CT continuum with respect to the exciton energy, which we label by index n. The total Hamiltonian of the studied system $H = H_0 + V$ with the perturbation operator $V = h + de^{-\imath\omega t} + Q$ describes the Fano interaction h between the exciton and CT continuum, the dipole interaction d with x-ray photons, and the Auger decay with the Coulomb operator Q. Thus, the total wave function of the system

$$\Psi = |0\rangle + a_n|cn\rangle + \int d\epsilon a_\epsilon|c\epsilon\rangle + b_n|fn\rangle + \int d\epsilon b_\epsilon|f\epsilon\rangle \tag{2}$$

obeys the Schrödinger equation $\imath(\partial_t + \Gamma\hat{)}\Psi = \tilde{V}\Psi$ in the interaction picture, where $\tilde{V} = e^{\imath H_0 t}Ve^{-\imath H_0 t}$. We neglect a small depopulation of the ground state $|0\rangle$. The solution of standard equations for the amplitudes of exciton (a_n) and CT (a_ϵ) core-excited states as well as for the amplitudes of exciton (b_n) and CT (b_ϵ) final double-core-hole excited states [20] provides the following expression for the differential cross section of the spectator RAS process $\sigma(\Omega, E) = \sigma_{\mathrm{exc}}(\Omega, E) + \sigma_{\mathrm{CT}}(\Omega, E) + \sigma_{\mathrm{int}}(\Omega, E)$ which is

the sum of exciton and CT contributions including $\sigma_{\rm int}(\Omega, E)$ describing the final-state interference between these RAS channels:

$$\sigma_{\rm exc}(\Omega, E) = \frac{c(1+q^2)(\Gamma_f+\gamma)\gamma}{[(\Omega-\Delta E_{\rm exc})^2+(\Gamma_f+\gamma)^2][\Omega^2+(\Gamma+\gamma)^2]},$$
$$\sigma_{\rm CT}(\Omega, E) = \frac{c(\Gamma+\Gamma_f)[(\Omega+q\gamma)^2+\Gamma^2]}{\Gamma[\Delta E_{\rm CT}^2+(\Gamma+\Gamma_f)^2][\Omega^2+(\Gamma+\gamma)^2]}. \quad (3)$$

Here, $c = 2\pi Q^2 d_{\epsilon 0}^2$, $\Delta E_{\rm exc} = E - E_{\rm exc}$ and $\Delta E_{\rm CT} = E - E_{\rm CT}$, $\gamma = \pi h_{\epsilon n}^2$ is the CT rate, q is the Fano shape parameter, $q^2 = D_{n0}^2/\pi\gamma d_{\epsilon 0}^2$, and $D_{n0} = d_{n0} - \int d\epsilon h_{n\epsilon} d_{\epsilon 0} (\epsilon-\Omega)/[(\epsilon-\Omega)^2+\Gamma^2]$ is the effective transition dipole moment of core excitation in the exciton state. We neglect the small difference between the transition matrix elements of the exciton and CT Auger decay channels $Q = Q_{cn,fn} \approx Q_{c\epsilon,f\epsilon}$. The Fano shift $q\gamma$ in the numerator of $\sigma_{\rm CT}(\Omega, E)$ describes the Fano interference of the exciton and CT in the core-excited state.

Importantly, the manifestation of final-state coherence in RAS differs qualitatively from the coherence observed in the core-excited state in XAS. Specifically, the stronger screening [27–30] of the $2p$ shell by localized excitons, compared to delocalized CT states, results in different Auger electron energies for these interfering final states [17] (Fig. 2). According to Bohr's complementarity principle, such which-path information quenches [31] the final-state interference between exciton and CT RAS channels, as we demonstrate below.

In many cases, including our experiment (see Fig. 2), the spacing $\Delta = E_{\rm exc} - E_{\rm CT}$ between resonant Auger energy of the exciton $E_{\rm exc}$ and the CT $E_{\rm CT}$ band is much larger than the lifetime broadening of the final state $\Delta \gg \Gamma_f$. The lifetime broadening Γ_f of the S $2p^{-2}$ final state is approximately three times larger [32] than the one of the S $2p^{-1}$ state ($\Gamma_{2p} = 0.05$ eV [33]). So, in our case $\Gamma_f \approx 0.15$ eV and $\Delta \approx 3$ eV. Therefore, contrary to the core-excited state, the Fano interference between the exciton and CT RAS channels in the final state is negligibly small $|\sigma_{\rm int}(\Omega, E)|/\sigma(\Omega, E) \sim 0.5 \times 10^{-2}$ [see Eqs. (11) and (12) in Ref. [20]].

The differential cross sections in Eq. (3) reproduce the experimentally observed dispersion laws of the exciton and CT RAS channels. The exciton cross section $\sigma_{\rm exc}(\Omega, E)$ follows a linear Raman dispersion of the Auger kinetic energy with photon energy $\Delta E_{\rm exc} = \Omega$, whereas for the CT cross section $\sigma_{\rm CT}(\Omega, E)$ the Auger kinetic energy is independent of the photon energy $\Delta E_{\rm CT} = 0$.

One can attempt to extract the CT time directly from the shape of the exciton differential cross section [34]. However, this method is limited to relatively simple systems, where vibrational and inhomogeneous broadening effects can be excluded. Analysis of CT in more complex systems requires a more robust and general method relying on the fundamental fingerprint of Fano interference as described below.

Integration of the differential cross sections in Eq. (3) over the Auger kinetic energy E results in the following expressions for the integral cross sections and their ratio:

$$\sigma_{\rm exc}(\Omega) = \pi c \frac{\gamma(1+q^2)}{\Omega^2+(\Gamma+\gamma)^2},$$
$$\sigma_{\rm CT}(\Omega) = \pi c \frac{[(\Omega+\delta)^2+\Gamma^2]}{\Gamma[\Omega^2+(\Gamma+\gamma)^2]},$$
$$f(\Omega) = \frac{\sigma_{\rm exc}(\Omega)}{\sigma_{\rm CT}(\Omega)} = \frac{\gamma\Gamma(1+q^2)}{(\Omega+q\gamma)^2+\Gamma^2} \overset{|q|=\infty}{\Rightarrow} \frac{\Gamma}{\gamma}, \quad (4)$$

where $\delta = q\gamma$ is the Fano interference shift. The ratio of the integral cross sections $f(\Omega)$ exhibits a Lorentzian dependence on the photon energy detuning Ω with a maximum at $\Omega = -\delta$. Assuming no direct excitation to the CT band (i.e., $d_{\epsilon 0} = 0$), the Fano shape parameter becomes infinitely large $|q| = \infty$, and the expression for $f(\Omega)$ reduces to the limiting case of CHC, where $f(\Omega) = \Gamma/\gamma$.

Figure 3 displays the integrated intensities of the σ^* exciton (red circles) and the CT π^* continuum (green triangles) extracted from fitting the experimental spectra using the SPANCF fitting suite for Igor Pro [35] (see the Supplemental Material [20] for more details). The ratio of these integrated intensities is shown as black squares. Data are plotted as a function of the detuning Ω, relative to the σ^* exciton resonance at $\omega_{\rm exc} = 2473.3$ eV.

Two key observations arise from the experimental data in Fig. 3. First, the integrated intensity of the CT π^* continuum shows a smooth Ω dependence, which has been previously observed in CT studies of extended systems with high density of unoccupied states with a smooth distribution of the oscillatory strength [12]. This behavior is attributed to the Fano continuum, resulting from the direct population of the CT band. This observation strongly contrasts with the conventional CHC theory, where the CT cross section is expected to replicate a sharp resonant behavior of the exciton resonance $\sigma_{\rm CT}(\Omega) = \sigma_{\rm exc}(\Omega)\gamma/\Gamma$. Second, the ratio of the integrated intensities exhibits a resonant dependence on Ω with the maximum shifted from the exciton resonance, occurring at $\Omega = 0$. This behavior aligns with our FCHC theory [Eq. (4)] and contradicts the CHC prediction of a constant ratio described by Eq. (1).

In the general case, the FCHC description of the CT process [Eq. (4)] depends on two unknown parameters—the CT rate γ and the Fano shape parameter q. By measuring the ratio of the integrated intensities at the exciton resonance $f \equiv f(\Omega = 0)$ and the Fano shift $\delta \equiv q\gamma$, we can directly extract the CT time from the experimental data. Substituting f and δ into Eq. (4), we obtain the following expression for γ (see the Supplemental Material [20] for details):

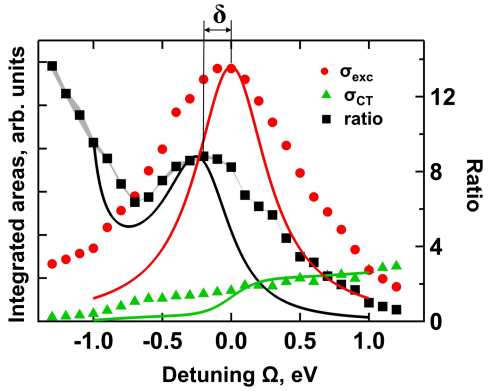

FIG. 3. Experimental integrated intensities of σ^* exciton $\sigma_{\mathrm{exc}}(\Omega)$ (circles), π^*-CT continuum $\sigma_{\mathrm{CT}}(\Omega)$ (triangles), and their ratio (squares). $\Omega = \omega - \omega_{\mathrm{exc}}$ is the detuning relative to the exciton peak of the P3HT polymer $\omega_{\mathrm{exc}} = 2473.3$ eV. Error bars resulting from the fit are within the marker size for $\sigma_{\mathrm{exc}}(\Omega)$ and $\sigma_{\mathrm{CT}}(\Omega)$ and are shown with the gray shaded area for their ratio. Solid lines show theoretical integral cross sections using Eq. (4) with $q = 17$, $\Gamma = 0.3$ eV, $\gamma = 0.012$ eV. The expression for $\sigma_{\mathrm{CT}}(\Omega)$ was multiplied by a linear function to account for the experimental background.

$$\gamma = \left(\frac{\delta^2 + \Gamma^2}{2\Gamma}\right) f - \sqrt{\left[\left(\frac{\delta^2 + \Gamma^2}{2\Gamma}\right) f\right]^2 - \delta^2}, \qquad (5)$$

where the S 1s lifetime broadening is $\Gamma = 0.3$ eV half width at half maximum [36] and the parameters $\delta = 0.2 \pm 0.01$ eV and $f = 8.24 \pm 0.06$ are determined from the data in Fig. 3. From this, we obtain the following values: $\gamma = 0.012$ eV, $q = \delta/\gamma = 17$, and the CT time $\tau_{\mathrm{CT}} = 0.658/2\gamma(\mathrm{eV}) = 27 \pm 1.8$ fs. To put this result in context, the obtained CT time should be compared with the CHC value of $\tau_{\mathrm{CT}} = 9 \pm 1$ fs for the P3HT polymer [17]. The finite value of the Fano parameter q indicates an important role of interference and provides unambiguous evidence that the case of the RAS in the P3HT polymer studied here falls outside the CHC regime, rendering Eq. (1) inapplicable.

The solid lines in Fig. 3 show the theoretical integral cross sections, calculated using Eq. (4) with $\Gamma = 0.3$ eV, $q = 17$, and $\gamma = 0.012$ eV. The expression for $\sigma_{\mathrm{CT}}(\Omega)$ was multiplied by a linear function to account for the experimental background. The theoretical curves show good qualitative agreement with the experimental data, especially considering that instrumental and vibrational broadening are not included in our model. Note, however, that according to our estimates the effect of possible instrumental and vibrational broadenings on the Fano shift δ is comparable to the quoted uncertainty of the fit and does not qualitatively affect the conclusions of the model (see the Supplemental Material [20] for more details). Furthermore, the experimental curves should be interpreted within a limited range around the exciton resonance, where $|\Omega| < 0.5$ eV, since at larger negative detunings, the CT signal begins to overlap with the lower-energy π^* exciton (Fig. 2).

In summary, we have developed a general quantum-mechanical Fano-based framework for timing ultrafast charge transfer by resonant Auger scattering and applied it to sulfur KLL Auger spectra of P3HT. Unlike the conventional CHC method, which assumes purely excitonic excitation, our approach accounts for the coherent population of both localized excitons and delocalized CT continua, giving rise to the Fano interference in the core-excited state. Our FCHC framework describes a general case of coherent exciton-continuum coupling and reduces to the limiting case of CHC when the Fano shape parameter becomes infinitely large and direct excitation to the CT continuum can be neglected.

High-resolution RAS measurements reveal two key signatures of this framework: a smooth photon-energy dependence of the CT channel, indicating direct population of the CT continuum, and a Fano-shifted resonance in the exciton-to-CT cross section ratio. These observations contradict the predictions of the conventional CHC. From the experimental data we extract both the CT time and the Fano shape parameter. A finite value of the Fano parameter $q = 17$ clearly demonstrates that the studied case lies beyond the CHC regime. Furthermore, the CT time $\tau_{\mathrm{CT}} = 27$ fs determined with FCHC strongly exceeds $\tau_{\mathrm{CT}} = 9$ fs obtained with CHC, demonstrating that CHC substantially underestimates CT times and highlighting a crucial role of direct population of the CT continuum.

Therefore, our results establish FCHC as a general and reliable approach for probing ultrafast charge transfer in molecules, polymers, and condensed-phase materials.

Acknowledgments—J.-C. L. thanks the National Natural Science Foundation of China (Grants No. 12541505 and No. 12211530044), and the Fundamental Research Funds for the Central Universities (Grant No. 2026JC012). N. V., T. M., and M. O. acknowledge funding from the European Union's Horizon 2020 research and innovation program under the Marie Skłodowska-Curie Grant Agreement No. [860553]. V. K. acknowledges Carl Tryggers Stiftelse (CTS) (Project No. 22:2077). P. K. acknowledges the Russian Science Foundation (Project No. 25-12-00148). We acknowledge SOLEIL for the provision of synchrotron radiation facilities, and we would like to thank the SOLEIL beamline staff for their assistance in using beamline GALAXIES under Proposals No. 20180196, No. 99210051 and No. 20201715. The computations were enabled by resources provided by the National Academic Infrastructure for Supercomputing in Sweden (NAISS), partially funded by the Swedish Research Council through Grant Agreement No. 2022-06725.

Data availability—The data that support the findings of this article are not publicly available. The data are available from the authors upon reasonable request.

[1] V. May and O. Kühn, *Charge and Energy Transfer Dynamics in Molecular Systems* (John Wiley & Sons, Hoboken, NJ, 2011), 10.1002/9783527633791.

[2] H. J. Wörner *et al.*, Charge migration and charge transfer in molecular systems, Struct. Dyn. **4**, 061508 (2017).

[3] U. Fano, Effects of configuration interaction on intensities and phase shifts, Phys. Rev. **124**, 1866 (1961).

[4] K. Kobayashi, H. Aikawa, S. Katsumoto, and Y. Iye, Tuning of the Fano effect through a quantum dot in an Aharonov–Bohm interferometer, Phys. Rev. Lett. **88**, 256806 (2002).

[5] K. L. Litvinenko, N. H. Le, B. Redlich, C. R. Pidgeon, N. V. Abrosimov, Y. Andreev, Z. Huang, and B. N. Murdin, The multi-photon induced Fano effect, Nat. Commun. **12**, 454 (2021).

[6] O. Björneholm, A. Nilsson, A. Sandell, B. Hernnäs, and N. Mårtensson, Determination of time scales for charge-transfer screening in physisorbed molecules, Phys. Rev. Lett. **68**, 1892 (1992).

[7] P. A. Brühwiler, O. Karis, and N. Mårtensson, Charge-transfer dynamics studied using resonant core spectroscopies, Rev. Mod. Phys. **74**, 703 (2002).

[8] F. Gel'mukhanov, M. Odelius, S. P. Polyutov, A. Föhlisch, and V. Kimberg, Dynamics of resonant x-ray and Auger scattering, Rev. Mod. Phys. **93**, 035001 (2021).

[9] F. Gel'mukhanov, P. Sałek, T. Privalov, and H. Ågren, Duration of x-ray Raman scattering, Phys. Rev. A **59**, 380 (1999).

[10] T. Marchenko, S. Carniato, L. Journel, R. Guillemin, E. Kawerk, M. Žitnik, M. Kavčič, K. Bučar, R. Bohinc, M. Petric, V. Vaz da Cruz, F. Gel'mukhanov, and M. Simon, Electron dynamics in the core-excited CS_2 molecule revealed through resonant inelastic x-ray scattering spectroscopy, Phys. Rev. X **5**, 031021 (2015).

[11] J. Stöhr, *The Nature of X-Rays and Their Interactions with Matter*, 1st ed. (Springer, New York, 2023).

[12] D. Menzel, Ultrafast charge transfer at surfaces accessed by core electron spectroscopies, Chem. Soc. Rev. **37**, 2212 (2008).

[13] A. Föhlisch, P. Feulner, F. Hennies, A. Fink, D. Menzel, D. Sanchez-Portal, P. M. Echenique, and W. Wurth, Direct observation of electron dynamics in the attosecond domain, Nature (London) **436**, 373 (2005).

[14] H. Ikeura-Sekiguchi and T. Sekiguchi, Attosecond electron delocalization in the conduction band through the phosphate backbone of genomic DNA, Phys. Rev. Lett. **99**, 228102 (2007).

[15] C. Arantes, B. G. A. L. Borges, B. Beck, G. Araújo, L. S. Roman, and M. L. M. Rocco, Femtosecond electron delocalization in poly(thiophene) probed by resonant Auger spectroscopy, J. Phys. Chem. C, **117**, 8208 (2013).

[16] F. O. L. Johansson, E. Berggren, L. M. Cornetta, D. Céolin, M. Fondell, H. Ågren, and A. Lindblad, Resonant Auger spectroscopy on solid xenon on gold, silver, and copper substrates, Phys. Rev. A **107**, 032802 (2023).

[17] N. Velasquez, F. B. Nunes, O. Travnikova, I. Ismail, R. Guillemin, J. B. Martins, D. Céolin, L. Journel, L. Fillaud, D. Koulentianos, C. Kamal, R. Püttner, M. N. Piancastelli, M. Simon, M. Odelius, M. Iannuzzi, and T. Marchenko, X-ray induced ultrafast charge transfer in thiophene-based conjugated polymers controlled by core-hole clock spectroscopy, Phys. Chem. Chem. Phys. **26**, 1234 (2024).

[18] E. Muchová, G. Gopakumar, I. Unger, G Öhrwall, D. Céolin, F. Trinter, I. Wilkinson, E Chatzigeorgiou, P. Slavíček, U. Hergenhahn, B. Winter, C. Caleman, and O. Björneholm, Attosecond formation of charge-transfer-to-solvent states of aqueous ions probed using the core-hole-clock technique, Nat. Commun. **15**, 8903 (2024).

[19] Y. Takata, T. Hatsui, and N. Kosugi, A unified view of resonant photoemission of metallic, molecular, and correlated solid systems, J. Electron Spectrosc. Relat. Phenom. **101–103**, 443 (1999).

[20] See Supplemental Material at http://link.aps.org/supplemental/10.1103/h6h9-j83r for the derivation of the resonant Auger scattering cross sections, characterization of charge-transfer dynamics induced with a short X-ray pulse, extraction of the charge-transfer rate and the Fano shape parameter from experiment, details of the data reduction and fitting procedures, and analysis of vibrational and inhomogeneous broadening effects, which includes Ref. [21].

[21] M. Abramowitz and I. Stegun, *Handbook of Mathematical Functions* (Dover Publications, INC., New York, 1972).

[22] A. J. Heeger, Nobel lecture: Semiconducting and metallic polymers: The fourth generation of polymeric materials, Rev. Mod. Phys. **73**, 681 (2001).

[23] D. Céolin, J. Ablett, D. Prieur, T. Moreno, J.-P. Rueff, T. Marchenko, L. Journel, R. Guillemin, B. Pilette, T. Marin, and M. Simon, Hard x-ray photoelectron spectroscopy on the GALAXIES beamline at the SOLEIL synchrotron, J. Electron Spectrosc. Relat. Phenom. **190**, 188 (2013).

[24] J.-P. Rueff, J. M. Ablett, D. Céolin, D. Prieur, T. Moreno, V. Balédent, B. Lassalle-Kaiser, J. E. Rault, M. Simon, and A. Shukla, The GALAXIES beamline at the SOLEIL synchrotron: Inelastic x-ray scattering and photoelectron spectroscopy in the hard x-ray range, J. Synchrotron Radiat. **22**, 175 (2015).

[25] Z.-F. Yao, Q.-Y. Li, H.-T. Wu, Y.-F. Ding, Z.-Y. Wang, Y. Lu, J.-Y. Wang, and J. Pei, Building crystal structures of conjugated polymers through x-ray diffraction and molecular modeling, SmartMat **2**, 378 (2021).

[26] U. Fano and J. W. Cooper, Spectral distributions of atomic oscillator strengths, Rev. Mod. Phys. **40**, 441 (1968).

[27] F. Gel'mukhanov and H. Ågren, Resonant inelastic x-ray scattering with symmetry-selective excitation, Phys. Rev. A **49**, 4378 (1994).

[28] H. Ågren, Y. Luo, F. Gel'mukhanov, and H. J. A. Jensen, Screening in resonant x-ray emission of molecules, J. Electron Spectrosc. Relat. Phenom. **82**, 125 (1996).

[29] P. Glans, P. Skytt, K. Gunnelin, J.-H. Guo, and J. Nordgren, Selectively excited x-ray emission spectra of N_2, J. Electron Spectrosc. Relat. Phenom. **82**, 193 (1996).

[30] P. Glans, K. Gunnelin, P. Skytt, J.-H. Guo, N. Wassdahl, J. Nordgren, H. Ågren, F. Kh. Gel'mukhanov, T. Warwick,

and E. Rotenberg, Resonant x-ray emission spectroscopy of molecular oxygen, Phys. Rev. Lett. **76**, 2448 (1996).
[31] J.-C. Liu, F. Gel'mukhanov, S. Polyutov, P. Krasnov, and V. Kimberg, Complementarity in which-path resonant Auger scattering, Phys. Rev. A **109**, 023116 (2024).
[32] M. Zitnik *et al.*, Two-to-one Auger decay of a double *L* vacancy in argon, Phys. Rev. A **93**, 021401(R) (2024).
[33] E. Kukk *et al.*, Orientational anisotropy due to molecular field splitting in sulfur 2p photoemission from CS_2 and SF_6—theoretical treatment and application to photoelectron recoil, Phys. Chem. Chem. Phys. **26**, 21810 (2024).
[34] F. Gel'mukhanov, F. O. L. Johansson, J.-C. Liu, M. Sanchis-Agudo, E. Cartwright, S. Polyutov, L. M. Cornetta, D. Céolin, M. Fondell, J. Wang, V. Kimberg, H. Ågren, and A. Lindblad, Direct x-ray probing of ultrafast charge transfer dynamics (to be published).
[35] E. Kukk, Spectrum Analysis by Curve Fitting (SPANCF) Macro Package for Igor Pro, 2009, http://www.geocities.ws/ekukk/intro.htm.
[36] M. O. Krause and J. H. Oliver, Natural widths of atomic *K* and *L* levels, $K\alpha$ x-ray lines and several *KLL* Auger lines, J. Phys. Chem. Ref. Data **8**, 329 (1979).